Original Article

Bone morphogenetic protein 4 ameliorates bleomycin-induced pulmonary fibrosis in mice by repressing NLRP3 inflammasome activation and epithelial-mesenchymal transition

Xin Xu[1,2,3#], Liang Yuan[3#], Xiao Hu[4#], Jingpei Li[1,2,3#], Huihui Wu[5#], Fang Chen[3], Fei Huang[1,2,3], Weiguo Kong[3], Wei Liu[3], Jingyi Xu[3], You Zhou[3], Yunhan Zou[3], Yi Shen[3], Ruijuan Guan[1,2,3*], Jianxing He[1,2,3*], Wenju Lu[3*]

[1]Department of Transplantation, Guangzhou Institute of Respiratory Health, the First Affiliated Hospital of Guangzhou Medical University, Guangzhou, China; [2]Department of Thoracic Surgery, Guangzhou Institute of Respiratory Health, the First Affiliated Hospital of Guangzhou Medical University, Guangzhou, China; [3]State Key Laboratory of Respiratory Disease, National Clinical Research Center for Respiratory Disease, Guangzhou Institute of Respiratory Health, the First Affiliated Hospital of Guangzhou Medical University, Guangzhou, China; [4]Institute of Basic Medical Sciences Chinese Academy of Medical Sciences, School of Basic Medicine Peking Union Medical College, Beijing, China; [5]Department of Endocrinology and Metabolism, Jing'an District Center Hospital of Shanghai, Shanghai, China

Contributions: (I) Conception and design: W Lu, J He, R Guan, X Xu; (II) Administrative support: X Xu; (III) Provision of study materials or patients: L Yuan, X Hu, J Li; (IV) Collection and assembly of data: L Yuan, X Hu, J Li, F Chen, H Wu, F Huang, W Kong, W Liu, J Xu, Y Zhou, Y Zou, Y Shen; (V) Data analysis and interpretation: X Xu, L Yuan, X Hu, J Li, H Wu; (VI) Manuscript writing: All authors; (VII) Final approval of manuscript: All authors.

[#]These authors contributed equally to this work as co-first authors.

[*]These authors contributed equally to this work.

Correspondence to: Wenju Lu, MD, PhD. State Key Laboratory of Respiratory Disease, National Clinical Research Center for Respiratory Disease, Guangzhou Institute of Respiratory Health, the First Affiliated Hospital of Guangzhou Medical University, No. 195 Dongfeng West Road, Yuexiu District, Guangzhou 510120, China. Email: wlu92@gzhmu.edu.cn; Jianxing He, MD, PhD; Ruijuan Guan, MD, PhD. Department of Transplantation, Guangzhou Institute of Respiratory Health, the First Affiliated Hospital of Guangzhou Medical University, No. 151 Yanjiang West Road, Yuexiu District, Guangzhou 510120, China; Department of Thoracic Surgery, Guangzhou Institute of Respiratory Health, the First Affiliated Hospital of Guangzhou Medical University, Guangzhou 510120, China; State Key Laboratory of Respiratory Disease, National Clinical Research Center for Respiratory Disease, Guangzhou Institute of Respiratory Health, the First Affiliated Hospital of Guangzhou Medical University, Guangzhou 510120, China. Email: drjianxing.he@gmail.com; 824171381@qq.com.

Background: Idiopathic pulmonary fibrosis (IPF) is a progressive and deadly lung disease with limited therapeutic options. Bone morphogenetic protein 4 (BMP4), a multifunctional growth factor that belongs to the transforming growth factor-β superfamily, is able to relieve pulmonary fibrosis in mice; nevertheless, the potential mechanism of action remains largely unknown. Growing evidence supports the notion that reiterant damage to the alveolar epithelial cells (AECs) is usually the "prime mover" for pulmonary fibrosis. Here, we examined the effect and mechanisms of BMP4 on bleomycin (BLM)-induced activation of NLR family pyrin domain containing 3 (NLRP3) inflammasome and epithelial-mesenchymal transition (EMT) *in vivo* and *in vitro*.

Methods: The *in vivo* impact of BMP4 was investigated in a BLM mouse model. Histopathologic changes were analyzed by hematoxylin-eosin (H&E) and Masson's trichrome staining. The NLRP3 inflammasome activation was determined by quantitative real time polymerase chain reaction (qRT-PCR) and immunofluorescence staining. Biomarkers of EMT were measured by qRT-PCR, Western blot and immunofluorescence staining. The *in vitro* impact of BMP4 on BLM-induced NLRP3 inflammasome activation and EMT was explored in A549 AECs. We also evaluated whether BMP4 inhibited BLM-activated ERK1/2 signaling to address the possible molecular mechanisms.

Results: BMP4 was significantly downregulated in the mouse lungs from BLM-induced pulmonary fibrosis. *BMP4*$^{+/-}$ mice presented with more severe lung fibrosis in response to BLM, and accelerated NLRP3

inflammasome activation and EMT process compared with that in *BMP4*$^{+/+}$ mice. Whereas overexpression of BMP4 by injecting adeno-associated virus (AAV) 9 into mice attenuated BLM-induced fibrotic changes, NLRP3 inflammasome activation, and EMT in the mouse lungs, thus exerting protective efficacy against lung fibrosis. *In vitro*, BMP4 significantly reduced BLM-induced activation of NLRP3 inflammasome and EMT in human alveolar epithelial A549 cells. Mechanically, BMP4 repressed BLM-induced activation of ERK1/2 signaling *in vivo* and *in vitro*, suggesting that ERK1/2 inactivation contributes to BMP4-induced effects on BLM-induced activation of NLRP3 inflammasome and EMT.

Conclusions: Our findings suggest that BMP4 can suppress NLRP3 inflammasome activation and EMT in AECs via inhibition of ERK1/2 signaling pathway, thus has a potential for the treatment of pulmonary fibrosis.

Keywords: Bone morphogenetic protein 4 (BMP4); pulmonary fibrosis; bleomycin (BLM); NLR family pyrin domain containing 3 inflammasome (NLRP3 inflammasome); epithelial-mesenchymal transition (EMT)

Submitted Dec 24, 2023. Accepted for publication Jun 11, 2024. Published online Aug 28, 2024.
doi: 10.21037/jtd-23-1947
View this article at: https://dx.doi.org/10.21037/jtd-23-1947

Introduction

Idiopathic pulmonary fibrosis (IPF), the most common type of idiopathic interstitial pneumonia, is usually a chronic, progressive, and fatal disease of unknown cause (1). Bleomycin (BLM), an antineoplastic drug widely used in cancer treatment, can cause pulmonary fibrosis and lead to respiratory failure. Intratracheal administration of BLM into mouse lungs also causes morphologic alteration in the pulmonary alveolar epithelium, which includes a loss of epithelial cells, an accumulation of extracellular matrix (ECM), and fibrosis (2). Increasing studies have shown that alveolar epithelial cells (AECs) contribute to the development of pulmonary fibrosis via epithelial-mesenchymal transition (EMT) induced phenotype transition (3,4). During EMT process, there is a decrease of intercellular adhesion and an incremental acquisition of migratory and invasive phenotype in mesenchymal cells with a production of ECM (4,5). Hence, identification of the molecular mechanism of EMT and its modulation are of interest as an underlying therapeutic target to attenuate lung fibrosis (6,7).

The presence of chronic inflammation also contributes to the development of IPF (8). It has been demonstrated that the pulmonary response to these inflammatory injuries is very important, as the lung must maintain its structural integrity for gas exchange (9). Inflammasomes are known as multiprotein complexes that play critical roles in innate immunity (10). The best characterized inflammasome is the NLR family pyrin domain containing 3 (NLRP3) inflammasome, consisting of NLRP3, apoptosis-associated speck-like protein containing a caspase recruitment domain (ASC), and the downstream molecule procaspase-1. Once NLRP3 inflammasome is being activated, it can promote the maturation of caspase-1 to secrete a mass of proinflammatory cytokines, such as IL-18 and IL-1β (11). Increasing evidence indicates that NLRP3 inflammasome is activated in IPF patients, as well as in asbestos-, silica-, PM2.5- and BLM-induced pulmonary fibrosis (8,12-15). NLRP3 inflammasome is also activated in AECs (for example, A549, MLE-12 and RLE-6TN cells) exposed to BLM (8,11). Interestingly, NLRP3 has also been illustrated to be involved in the modulation of EMT process in experimental lung fibrosis (11). Therefore, anti-inflammatory therapy via regulating NLRP3 contributes to the inhibition of EMT process and serves as a potential treatment strategy of IPF.

Bone morphogenetic proteins (BMPs) are a huge subgroup of ligands belonging to the transforming growth factor (TGF)-β superfamily (16). The balance between BMP and TGF-β signaling has significant meaning during the course of lung development and regeneration (17). BMP4, a member of the BMPs family, regulates multiple physiological functions, for example, oxidative stress, inflammation, proliferation, and differentiation of different types of cells in the body (18-20). It has been reported that BMP4 suppresses EMT in multiple cell lines including lens epithelial cells and retinal pigment epithelium (RPE) cells (17,21). BMP4 regulates browning of perivascular

adipose tissue, reduces endothelial inflammation and prevents atherosclerosis (22). Our previous research has shown that BMP4 deficiency accelerates cellular senescence and defective mitophagy of lung fibroblasts and promotes lung fibrosis in mice (23). However, it remained uncertain whether BMP4 directly affects BLM-induced activation of NLRP3 inflammasome and EMT phenotype in AECs. In the present study, we found BMP4 was strongly downregulated in BLM-induced lung injury. BMP4 haploinsufficiency mice developed more grievous lung injury and interstitial fibrosis, NLRP3 inflammasome activation, and EMT after BLM. While mice treated with an adeno-associated virus serotype 9 vector expressing BMP4 (AAV9-BMP4) exhibited the overexpression of BMP4 in the lung and thus showed protective efficacy against lung fibrosis, NLRP3 inflammasome activation, and EMT. Additionally, BMP4 attenuated BLM-induced activation of NLRP3 inflammasome and EMT in alveolar A549 cells. Moreover, we clarified that the protective role of BMP4 is related to the inactivation of ERK1/2 signaling pathway. Collectively, these data suggest that BMP4 alleviates BLM-induced lung fibrosis by affecting NLRP3 inflammasome activation and EMT in AECs via ERK1/2 signaling pathway, thus leading to a novel therapeutic approach to treat fibrotic lung diseases. We present this article in accordance with the ARRIVE reporting checklist (available at https://jtd.amegroups.com/article/view/10.21037/jtd-23-1947/rc).

Highlight box

Key findings

- Our study confirms that in bleomycin-induced lung fibrosis, bone morphogenetic protein 4 (BMP4) exerts its anti-fibrotic effects by regulating NLR family pyrin domain containing 3 (NLRP3) inflammasome activation and epithelial-mesenchymal transition (EMT) process in alveolar epithelial cells (AECs) via ERK1/2 signaling pathway.

What is known and what is new?

- EMT contributes to the development of pulmonary fibrosis. In addition, NLRP3 inflammasome is activated and participates in the modulation of EMT in pulmonary fibrosis. BMP4 inhibits BLM-induced cellular senescence and mitophagy deficiency in lung fibroblasts.
- We confirm that BMP4 inhibits pulmonary fibrosis by regulating NLRP3 inflammasome activation and EMT process in AECs via ERK1/2 signaling pathway.

What is the implication, and what should change now?

- Our findings suggest that BMP4 can inhibit NLRP3 inflammasome activation and EMT in AECs via ERK1/2 signaling, thus maybe potentially used in the treatment of pulmonary fibrosis. This study may provide a new option for the treatment of pulmonary fibrosis. However, further exploration is needed to determine whether BMP4 can be applied to the treatment of pulmonary fibrosis in clinical practice.

Methods

Reagents and antibodies

BLM was purchased from Nippon Kayaku (Tokyo, Japan). Anti-NLRP3, anti-ASC, anti-Caspase-1 and anti-SFTPC antibodies were obtained from ABclonal Technology (Wuhan, Hubei, China). Anti-E-cadherin, anti-vimentin, anti-p-ERK1/2 and anti-ERK1/2 antibodies were obtained from CST (Danvers, MA, USA). Anti-β-actin antibody, and the horseradish peroxidase (HRP)-labeled second antibodies were obtained from Abcam (Cambridge, MA, USA).

Animals and experiment design

BMP4$^{+/-}$ mice with C57BL/6J background were provided by Jackson Laboratory (Bar Harbor, Maine, USA). Since homozygous *BMP4*$^{-/-}$ is lethal to the embryos, heterozygous *BMP4*$^{+/-}$ mice were used to observe the fibrotic response to BLM injury (19,23). These mice were maintained in a specific pathogen-free room with free access to food and water. The *BMP4*$^{+/-}$ or wide type (WT) mice were randomly divided into control (CTL) or BLM groups, respectively. To induce pulmonary damage, *BMP4*$^{+/-}$ or WT mice (6–8 weeks old, weighing 20–25 g) were anaesthetized with 1.2% Avertin solution (20 g/350 μL) and then received an intratracheal injection of BLM (2.0 mg/kg body weight) or equivalent saline as described previously (23). On day 21 after the intratracheal drip of BLM, lungs were harvested for the following analysis. There were 6 mice per group for this experiment.

To further confirm the role of BMP4 in lung fibrosis, separate batches of C57BL/6J mice (6–8 weeks old, weighing 20–25 g) were purchased from Hunan SJA Laboratory Animal Co., Ltd (Changsha, China) for the following experiments. These mice were randomly divided into Control, BLM+ AAV9-GFP and BLM+ AAV9-BMP4 groups. Mice were anesthetized by 1.2% Avertin solution (20 g/350 μL) and BLM was injected intratracheally at a concentration of 2.5 mg/kg or saline as controls as described previously (23). These mice were then treated with BMP4-expressing AAV9 viral (PackGene Biotech, Guangzhou,

China) on day 10 after the intratracheal drip of BLM. Identical doses of AAV9-GFP virus were used as controls. There were 5–7 mice per group for this experiment.

For the animal experiments above, only the experimenter knew the grouping. In addition, a protocol for animal experiments was prepared before the study with registration in the Animal Care and Use Committee of Guangzhou Medical University. Animal experiments were performed under a project license (No. 2021433) granted by the Animal Care and Use Committee of Guangzhou Medical University, in compliance with institutional guidelines for the care and use of animals.

Histology analysis

Left lungs were fixed with 10% neutral formalin for 48 h, dehydrated with gradient alcohol and embedded with paraffin. These paraffin-embedded lung samples were cut into 5 μm-thick lung sections, and then stained with hematoxylin and eosin (H&E) or Masson's trichrome staining for morphological assessment. The histologic sections were photographed using light microscopy (Pannoramic SCAN, 3DHISTECH Ltd., Hungary). The degree of pulmonary fibrosis was determined by semi-quantitative analysis methods described by Ashcroft and Simpson (24).

Cell culture

Human type II alveolar A549 cells were provided by Cell Bank of the Chinese Academy of Sciences (Shanghai, China), and cultured in Dulbecco's modified Eagle's medium (DMEM, Procell, Wuhan, China) containing 10% fetal bovine serum (FBS, Thermo Fisher Scientific, Waltham, MA, USA) and 1% penicillin-streptomycin (Solarbio, Beijing, China) in a humidified incubator at 37 ℃ with 5% CO_2 humidified atmosphere. A549 cells were stimulated with BLM (50 μg/mL) for 48 h in the presence and absence of BMP4 in six- or twelve-well plates. Each cell experiment was repeated three times.

Immunofluorescence staining

Tissue immunofluorescence staining was performed with a multiplex fluorescence kit (AiFang Biological, Changsha, China) using the tyramide signal amplification (TSA) principle. Briefly, lung sections of 5 μm thickness were deparaffinized, rehydrated, and antigen retrieval in citrate buffer antigen repair solution (pH 6.0, Servicebio, Wuhan, China) with microwave oven. After washing three times with phosphate buffer saline (PBS, Biosharp, Beijing, China) containing 0.1% Tween-20 (Solarbio), protein blocking was performed using 3% H_2O_2 solution (Biosharp) for 15 min and goat serum for 30 min before every staining cycle. Primary antibodies against SFTPC (SPC, 1:500 dilution), vimentin (1:500 dilution), Caspase-1 (1:500 dilution), ASC (1:500 dilution), and NLRP3 (1:500 dilution) were used to the lung sections respectively for 12 h at 4 ℃. Then HRP-labeled rabbit secondary antibody was used to the lung sections for 30 min, followed by incubation with TSA opal fluorophore for 10 min at room temperature. After washing three times with PBST, the lung sections were counterstained with 2-(4-Amidinophenyl)-6-indolecarbamidine dihydrochloride (DAPI, Beyotime Biotechnology, Shanghai, China). The immunofluorescence images were captured with a fluorescence microscope (DM6, Leica, Wetzlar, Germany).

Cellular immunofluorescence was performed as described previously (25). Briefly, alveolar A549 cells were seeded on sterile glass slides in a 12-well plate and incubated with BLM (50 μg/mL) for 48 h in the presence and absence of BMP4. These slides were subsequently washed with PBS for three times, fixed in 4% paraformaldehyde for 10 min, and blocked with 3% bovine serum albumin (BSA, Biosharp) at room temperature for 1 h. These fixed A549 cells were incubated overnight at 4 ℃ with corresponding primary antibodies, followed by 1 h at room temperature with the goat anti-rabbit Cy3 (red)-conjugated antibody secondary antibody (1:400 dilution, Beyotime Biotechnology). After washing three times with PBS, the nuclei were stained with DAPI. Images were obtained with a fluorescent microscope (DM6). Primary antibodies used were anti-NLRP3 (1:200 dilution), and anti-Caspase 1 (1:200 dilution).

Quantitative real-time polymerase chain reaction analysis (qRT-PCR)

Total RNA was extracted using Trizol reagent (Invitrogen Corporation, Carlsbad, CA, USA). cDNA was obtained by reverse transcription using a Color Reverse Transcription Kit (EZBioscience, Roseville, MN, USA). The mRNA expression levels were analyzed by qRT-PCR with the above cDNA using qPCR SYBR Green Master Mix (Yeasen, Shanghai, China). Relative mRNA levels the of target genes were examined by normalizing the values to 18s mRNA levels. The primers for the real-time PCR are listed in *Table 1*.

Table 1 qRT-PCR primer sequence

Gene name	Forward (5'-3')	Reverse (5'-3')
BMP4 (m)	TTGATACCTGAGACCGGGAAG	ACATCTGTAGAAGTGTCGCCTC
COL1A1 (m)	CTGGCGGTTCAGGTCCAAT	TTCCAGGCAATCCACGAGC-3
COL1A2 (m)	AAGGGTGCTACTGGACTCCC	TTGTTACCGGATTCTCCTTTGG
Snail (m)	GGAGTTGACTACCGACCTTGC	CTGGAAGGTGAACTCCACACAC
MMP2 (m)	GCCCCCATGAAGCCTTGTTT	ATAGCGGTCTCGGGACAGAA
MMP9 (m)	TCACCATGAGTCCCTGGCA	AGCGGTACAAGTATGCCTCTGC
MMP12 (m)	TCTGCTGAAAGGAGTCTGCAC	AGGTTTCTGCTGGGAACCTTCAG
NLRP3 (m)	ATTACCCGCCCGAGAAAGG	CATGAGTGTGGCTAGATCCAAG
ASC (m)	GACAGTGCAACTGCGAGAAG	CGACTCCAGATAGTAGCTGACAA
CASP1 (m)	ACAAGGCACGGGACCTATG	TCCCAGTCAGTCCTGGAAATG
18s	GCAATTATTCCCCATGAACG	GGCCTCACTAAACCATCCAA

qRT-PCR, quantitative real time polymerase chain reaction.

Western blot

Western blot was performed as described previously. Briefly, lung tissues or alveolar A549 cells were lysed in ice-cold RIPA containing phosphatase inhibitor and then centrifuged to gain the supernatants. Total protein concentration was detected using a bicinchoninic acid (BCA) protein analysis kit (Beyotime Biotechnology). Equal amounts of protein (20 μg) were loaded into each lane onto 10% sodium dodecyl sulfate-polyacrylamide (SDS)-polyacrylamide gels, and subsequently transferred to poly-vinylidene fluoride (PVDF) membranes (Millipore Corporation, Billerica, MA, USA) and incubated overnight at 4 ℃ with the primary antibodies against E-cadherin, vimentin, NLRP3, ASC, Caspase-1, p-ERK1/2, ERK1/2, and β-actin. β-actin was used as the internal control. On the following day, these membranes were washed with tris-buffered saline containing 0.1% Tween-20 (TBST) buffer and incubated with HRP-labeled secondary antibodies for 1 h at room temperature. After washing three times with TBST buffer, the target bands were visualized using an ECL detection kit (Tanon Science & Technology Co., Ltd., Shanghai, China) using Tanon-5200 (Shanghai Tianneng Life Science Co, Shanghai, China). The results were analyzed by Image J.

Data and statistical analysis

Data analysis was performed using GraphPad Prism 6.0 (San Diego, CA, USA), and was expressed as means ± standard error of mean (SEM). Student's *t*-test (for two value sets) or one-way analysis of variance (one-way ANOVA, for multiple groups) was applied to investigate statistical significance. A two-sided P value of <0.05 was considered to be significantly different.

Results

Effects of BMP4 deficiency on BLM-induced pulmonary fibrosis

BMP4 expression was significantly decreased in lungs of C57BL/6 mice after BLM-induced injury compared with uninjured controls (*Figure 1A*,*1B*). Also, as compared to WT mice, *BMP4*$^{+/-}$ mice showed a remarkably exaggerated inflammatory and fibrotic responses to low doses of BLM as demonstrated by enhanced H&E (*Figure 1C*,*1D*) and Masson's trichrome staining (*Figure 1E*,*1F*), and higher mRNA levels for COL1A1 and COL1A2 (*Figure 1G*,*1H*) in the lungs after BLM. Increased ACTA2 mRNA (encoding α-SMA) expression (*Figure 1I*) was also found in the lungs of *BMP4*$^{+/-}$ mice as compared to that in WT mice, implying the increase of myofibroblasts. These data imply that BMP4 deficiency promotes pulmonary fibrogenesis in mice.

Effects of BMP4 overexpression on BLM-induced pulmonary fibrosis

Encouraged by our findings, we therefore explored whether

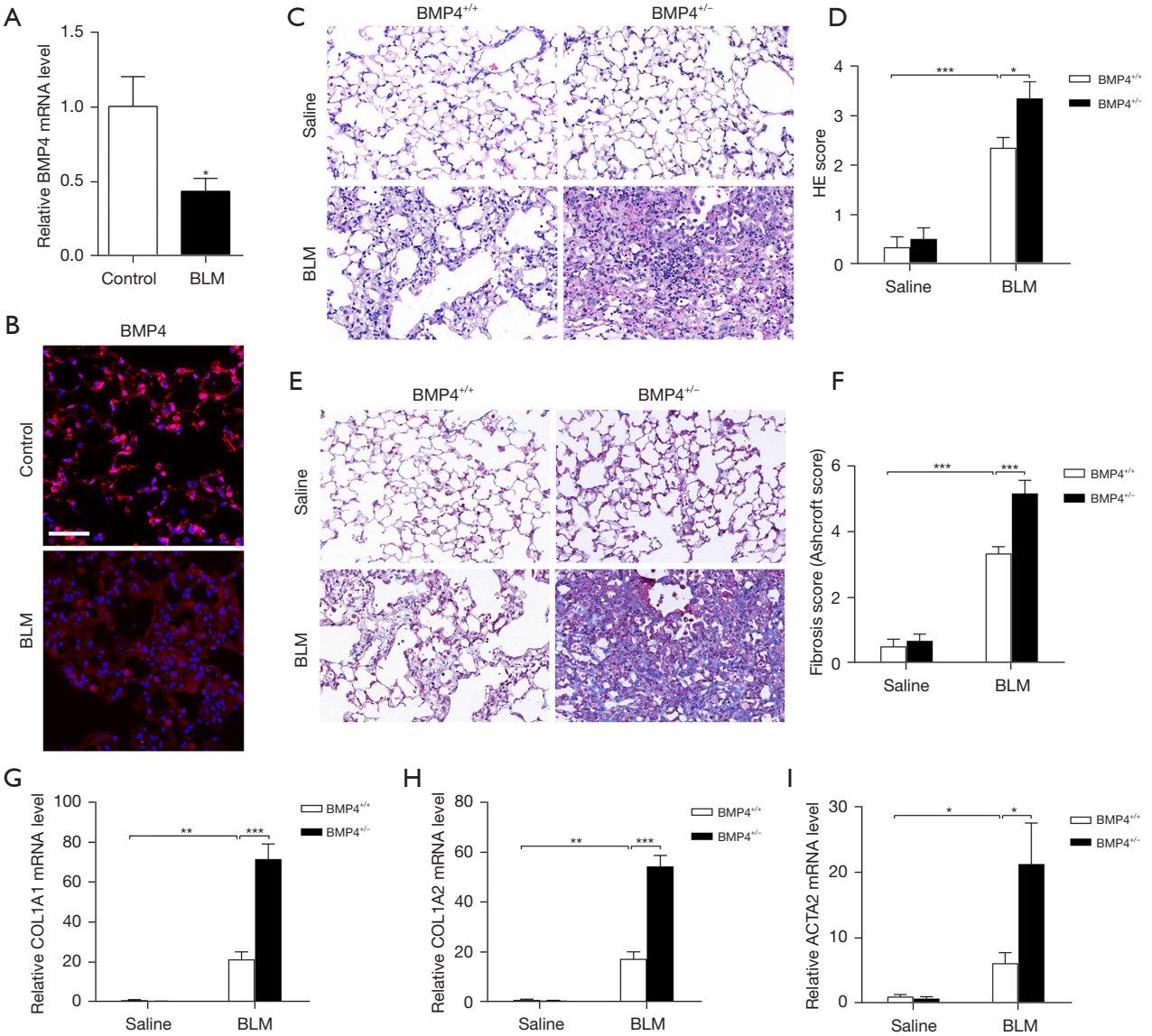

Figure 1 Effects of BMP4 deficiency on BLM-induced pulmonary fibrosis. BMP4 expression in the lungs of saline and BLM-treated mouse (day 21) as assessed by qRT-PCR (A) and immunofluorescence (B). Data are presented as the mean ± SEM, n=6. Scale bar, 100 μm. *BMP4*$^{+/-}$ and *BMP4*$^{+/+}$ mice were challenged with intratracheal BLM and analyzed after 21 days. Representative H&E (C) and Masson trichrome staining (E) of lung tissues after BLM treatment. Original magnification, ×200. (D,F) Histopathological grading of inflammation and fibrosis were assessed. Data are presented as the mean ± SEM, n=6. (G-I) qRT-PCR analysis of COL1A1, COL1A2, and ACTA2 mRNA levels in lung homogenates of BLM-challenged *BMP4*$^{+/+}$ and *BMP4*$^{+/-}$ mice. Data are presented as the mean ± SEM, n=4–5. *, P<0.05; **, P<0.01; ***, P<0.001. BLM, bleomycin; H&E, hematoxylin-eosin; qRT-PCR, quantitative real time polymerase chain reaction; SEM, standard error of mean.

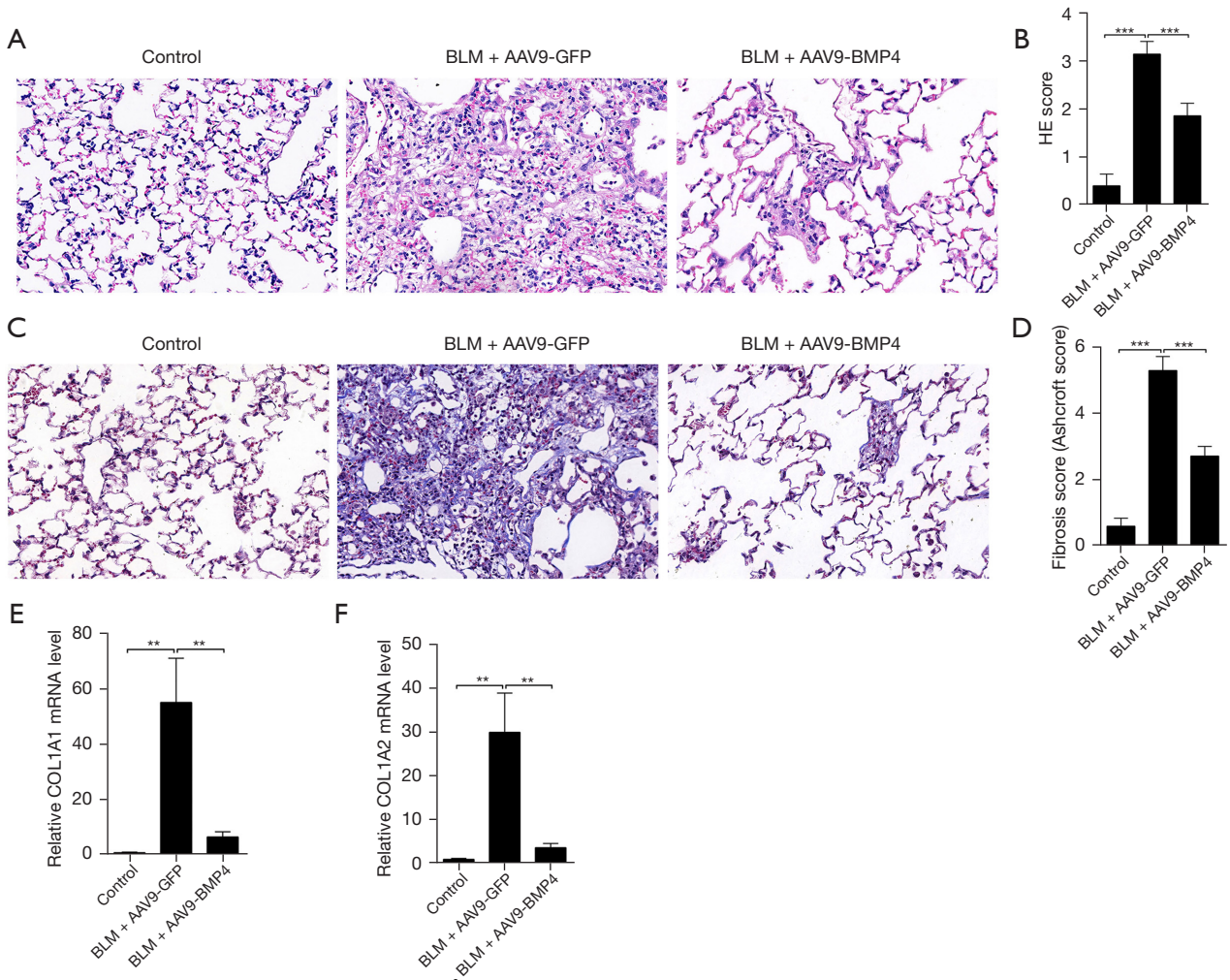

Figure 2 Effects of BMP4 overexpression on BLM-induced pulmonary fibrosis. Mice were intratracheally injected with BLM, and were subsequently intratracheally injected with AAV9-BMP4 or AAV9-GFP on day 10. Representative H&E (A) and Masson trichrome staining (C) of lung sections from AAV9-BMP4- or AAV9-GFP-treated mice. Original magnification, ×200. (B,D) Histopathological grading of inflammation and fibrosis were assessed. (E,F) qRT-PCR analysis of COL1A1, and COL1A2 mRNA levels in the lungs of AAV9-BMP4- or AAV9-GFP-treated mice. Data are presented as the mean ± SEM, n=5–7. **, P<0.01; ***, P<0.001. BLM, bleomycin; H&E, hematoxylin-eosin; qRT-PCR, quantitative real time polymerase chain reaction; SEM, standard error of mean.

overexpression of BMP4 in the lung could attenuate the BLM-induced lung fibrosis. The results showed that overexpression of BMP4 using AAV9 virus significantly attenuated BLM-induced pulmonary fibrosis as indicated by H&E staining (*Figure 2A,2B*), and Masson's trichrome staining (*Figure 2C,2D*). In line with the morphological changes, mice overexpressing BMP4 showed a significant reduction in COL1A1 and COL1A2 mRNA levels (*Figure 2E,2F*).

Effects of BMP4 on BLM-induced activation of NLRP3 inflammasome in mice

A previous study has demonstrated that NLRP3 inflammasome activation promoted pulmonary fibrosis in mice (8). Hence, we first explored the role of BMP4 deficiency in BLM-induced activation of NLRP3 inflammasome in the mouse lungs. As shown in *Figure 3A-3C*, the mRNA levels of NLRP3, ASC, and Caspase-1 were significantly upregulated in BLM group, which were

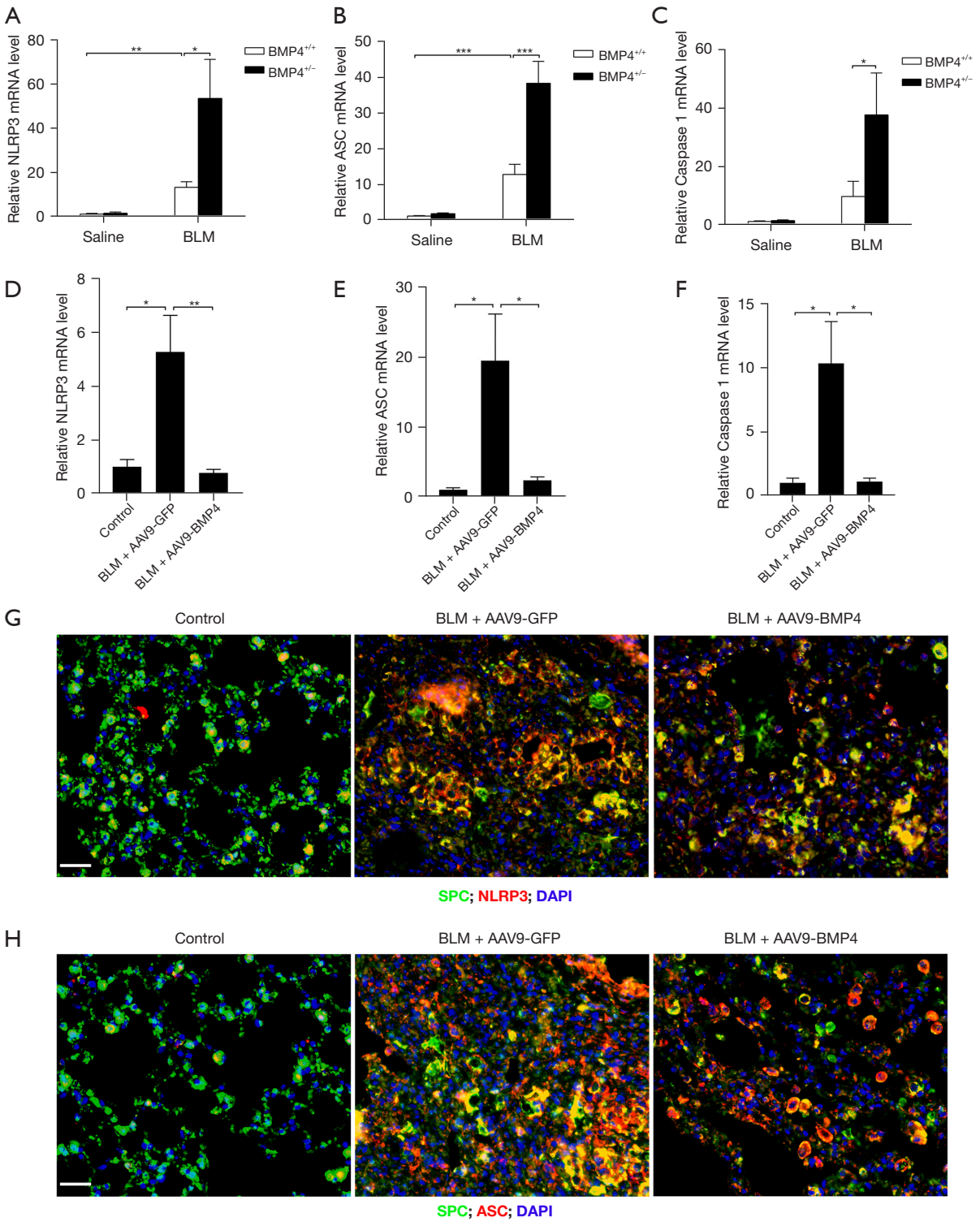

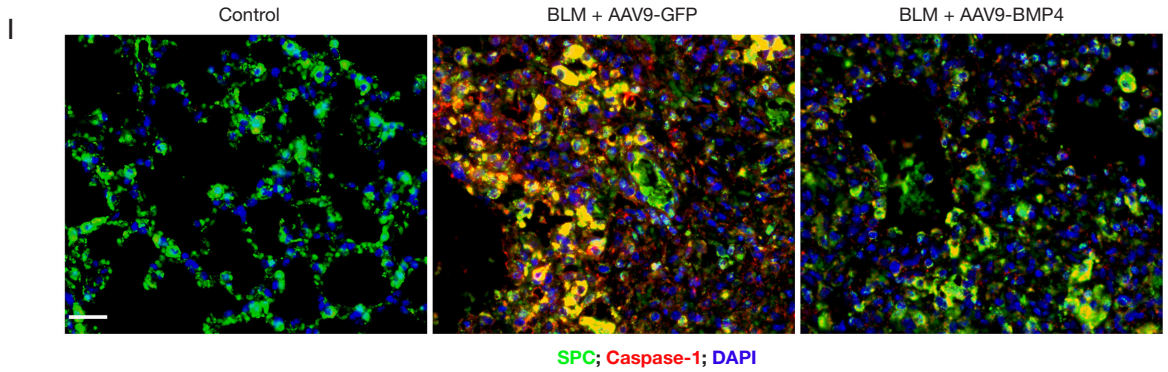

Figure 3 Effects of BMP4 on BLM-induced NLRP3 inflammasome activation in mice. (A-C) *BMP4*$^{+/+}$ and *BMP4*$^{+/-}$ mice were challenged with intratracheal BLM and analyzed after 21 days. qRT-PCR analysis of NLRP3, ASC, and Caspase-1 mRNA levels in the lungs of BLM-challenged *BMP4*$^{+/+}$ and *BMP4*$^{+/-}$ mice. Data are presented as the mean ± SEM, n=4–5. Mice were intratracheally injected with BLM, and were subsequently intratracheally injected with AAV9-BMP4 or AAV9-GFP on day 10. (D-F) qRT-PCR analysis of NLRP3, ASC, and Caspase-1 mRNA levels in the lungs of AAV9-BMP4- or AAV9-GFP-treated mice. Data are presented as the mean ± SEM, n=5–7. (G-I) Immunofluorescence analysis of NLRP3, ASC and Caspase-1 expressions in lung sections (nucleus, DAPI). Representative images of the staining are shown. Scale bar, 25 μm. *, P<0.05; **, P<0.01; ***, P<0.001. BLM, bleomycin; qRT-PCR, quantitative real time polymerase chain reaction; SEM, standard error of mean.

further enhanced by BMP4 haploinsufficiency, indicating BMP4 haploinsufficiency enhanced BLM-induced NLRP3 inflammasome activation in mice. Next, we investigated whether overexpression of BMP4 could inhibit BLM-induced NLRP3 inflammasome activation in the lungs. Likewise, the BLM-induced increased mRNA levels of NLRP3, ASC and Caspase-1 were also significantly attenuated by BMP4 overexpression (*Figure 3D-3F*). Further, multiplex immunofluorescence assay showed that the BLM-induced upregulation of NLRP3, ASC and Caspase-1 in the AECs (co-localizing with the AECs marker SPC) was decreased by BMP4 overexpression (*Figure 3G-3I*). These findings confirm that BMP4 repressed NLRP3 inflammasome activation in BLM-treated mice.

Effects of BMP4 on BLM-induced EMT in mice

EMT, which is mediated by NLRP3 inflammasome, is a critical stage during the development of pulmonary fibrosis (8). We therefore investigated whether BMP4 deficiency aggravated the lung fibrosis by increasing EMT. Western blot assay showed that E-cadherin expression was decreased, but vimentin expression was increased (*Figure 4A*,*4B*), suggesting BLM-induced EMT in the mouse lungs. However, the BLM-induced downregulation of E-cadherin and upregulation of vimentin in *BMP4*$^{+/-}$ mice was dramatically increased, which implicates *BMP4*$^{+/-}$ mice display increased EMT after BLM treatment (*Figure 4A*,*4B*).

We then investigated whether overexpression of BMP4 attenuated BLM-induced EMT in mouse lungs. Western blot analysis showed that AAV9-mediated overexpression of BMP4 in this mouse model showed an obvious increase of E-cadherin protein level, as well as a significant decrease of vimentin level, in comparison with the BLM-stimulated mice (*Figure 4C*,*4D*). This apparent EMT phenomenon was also confirmed by the presence of SPC/vimentin double positive cells, reflecting their epithelial origin and a possible intermediate transitional stage of EMT (*Figure 4E*). Impressively, the amount of epithelial-derived fibroblasts and the protein expression levels of vimentin were both decreased by BMP4 overexpression, indicating that BMP4 inhibited the BLM-induced EMT process *in vivo* (*Figure 4E*). Since EMT can be driven by Snail transcription factor, we also explored its expression after BMP4 overexpression. We found that the BLM-induced elevation of Snail was significantly decreased by BMP4 overexpression (*Figure 4F*). Additionally, the BLM-induced upregulation of MMP2, MMP9 and MMP12 (*Figure 4G-4I*), proteolytic enzymes that positively correlate with EMT, was also attenuated by BMP4 overexpression. All these findings further support the

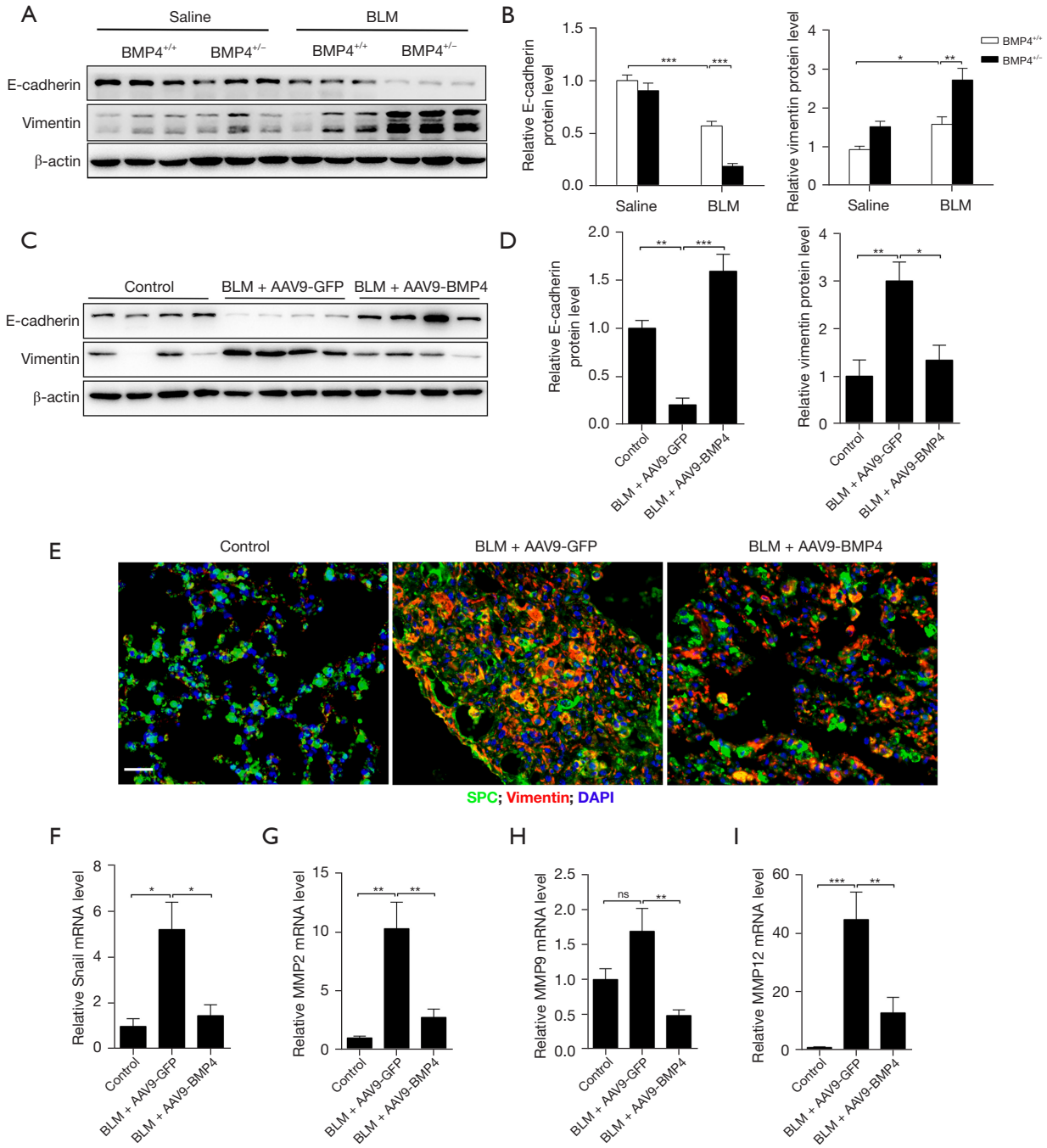

Figure 4 Effects of BMP4 on BLM-induced EMT in mice. (A,B) *BMP4*$^{+/+}$ and *BMP4*$^{+/-}$ mice were challenged with intratracheal BLM and analyzed after 21 days. Western blot analysis of E-cadherin and vimentin in lung homogenates of BLM-challenged *BMP4*$^{+/+}$ and *BMP4*$^{+/-}$ mice. β-actin was used as a loading control. Data are presented as the mean ± SEM, n=6. Mice were intratracheally injected with BLM, and were subsequently intratracheally injected with AAV9-BMP4 or AAV9-GFP on day 10. (C,D) Western blot analysis of E-cadherin and vimentin in lung homogenates of AAV9-BMP4- or AAV9-GFP-treated mice. Data are presented as the mean ± SEM, n=4. (E) The levels of SPC and vimentin were visualized using immunofluorescence staining in the lungs of AAV9-BMP4- or AAV9-GFP-treated mice. Scale bar, 25 μm. (F-I) qRT-PCR analysis of Snail, MMP2, MMP9, and MMP12 mRNA levels in the lungs of AAV9-BMP4- or AAV9-GFP-treated mice. Data are presented as the mean ± SEM, n=5–7. ns means not significant; *, P<0.05; **, P<0.01; ***, P<0.001. BLM, bleomycin; EMT, epithelial-mesenchymal transition; qRT-PCR, quantitative real time polymerase chain reaction; SEM, standard error of mean.

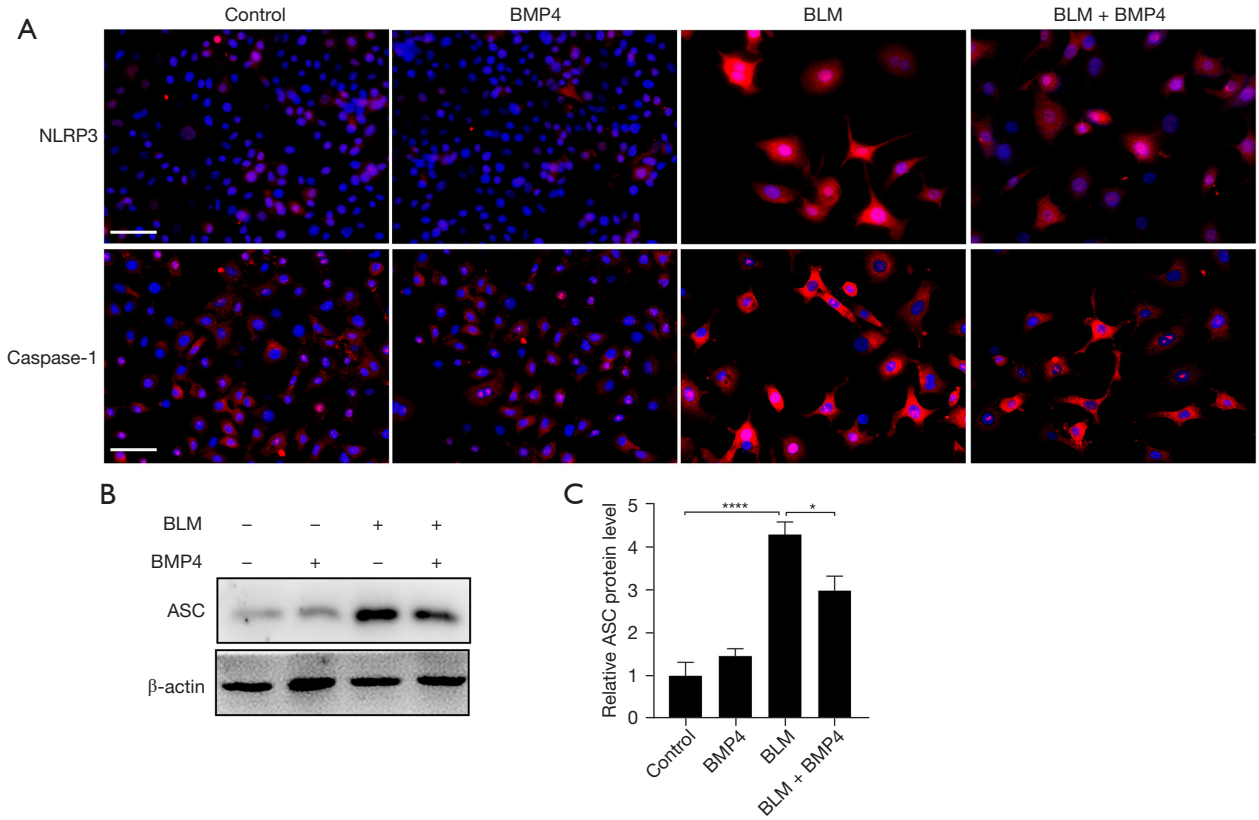

Figure 5 Effects of BMP4 on BLM-induced NLRP3 inflammasome activation in alveolar epithelial A549 cells. A549 cells were treated with BLM (50 μg/mL, 48 h) in the presence of BMP4 or vehicle. (A) NLRP3 and Caspase-1 were examined by immunofluorescence. Representative images of the staining are shown. Scale bar, 50 μm. (B) Western blot analysis was performed to measure the protein level of ASC. (C) Densitometric analysis of ASC protein in the immunoblots using β-actin as the internal reference. Data are presented as the mean ± SEM, n=3. *, P<0.05; ****, P<0.0001. BLM, bleomycin; SEM, standard error of mean.

notion that BMP4 represses EMT in BLM-treated mice.

Effects of BMP4 on BLM-induced NLRP3 inflammasome activation in alveolar A549 cells

Since AECs, especially type II AECs, are important players in IPF (26), and NLRP3 is not only present but also activated in AECs (11,27), we explored the impact of BMP4 on BLM-induced activation of NLRP3 inflammasome in alveolar A549 cells. Immunofluorescence staining showed that BLM stimulation increased the expression levels of NLRP3 and Caspase-1 in type II AECs, which were decreased by BMP4 treatment (*Figure 5A*). In addition, as shown in *Figure 5B,5C*, BLM significantly elevated the protein level of ASC, which was reduced by BMP4 treatment. These data suggested BMP4 suppresses BLM-induced NLRP3 inflammasome activation in AECs *in vitro*.

Effects of BMP4 on BLM-induced EMT in alveolar A549 cells

We also investigated the impact of BMP4 on BLM-induced the emergence of EMT in AECs *in vitro*. Likewise, BMP4 significantly suppressed BLM-induced EMT process in alveolar A549 cells, as indicated by the protein expression levels of EMT-related protein biomarkers (*Figure 6A,6B*).

Effects of BMP4 on BLM-induced ERK1/2 signaling activation in vivo and in vitro

We examined the activation status of ERK1/2 signaling in the lungs of BLM-treated *BMP4*$^{+/-}$ and WT mice *in vivo* by performing Western blot of p-ERK1/2. Compared with the control lungs, the level of p-ERK1/2 was obviously up-regulated in BLM-induced mouse lungs, indicating the

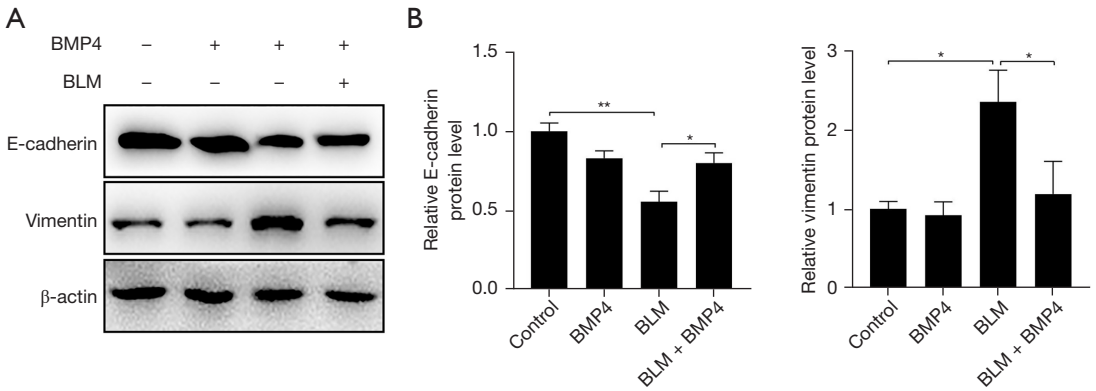

Figure 6 Effects of BMP4 on BLM-induced EMT in alveolar epithelial A549 cells. (A) Western blot analysis of E-cadherin and vimentin in total cell lysates of A549 cells treated with BLM (50 μg/mL, 48 h) in the presence of BMP4 or vehicle. (B) Densitometric analysis of relevant proteins in the immunoblots using β-actin as the internal reference. Data are presented as the mean ± SEM, n=3. *, P<0.05; **, P<0.01. BLM, bleomycin; EMT, epithelial-mesenchymal transition; SEM, standard error of mean.

activation of ERK1/2 signaling in BLM mice. Nevertheless, haploinsufficiency of BMP4 significantly enhanced the levels of p-ERK1/2 (*Figure 7A*). Inversely, BMP4 overexpression dramatically decreased the levels of p-ERK1/2 (*Figure 7B*). Moreover, BMP4 also reduced BLM-induced upregulation of p-ERK1/2 in alveolar A549 cells (*Figure 7C*). These results suggest an inhibitory effect of BMP4 on BLM-induced activation of ERK1/2 signaling *in vivo* and *in vitro*.

Discussion

IPF is a refractory interstitial lung disease, characterized by the aberrant accumulation of ECM composition after lung injury, which eventually causes respiratory failure (28). It is a major health problem affecting ~5 millions of people worldwide and its incidence rate increases with age (29). Currently, treatment of lung fibrosis is very limited and often ineffective, due to the lack of comprehensive understanding of the molecular mechanisms of lung fibrosis (30). BLM is a chemotherapeutic agent widely used for multiple cancers in clinic and its adverse drug reactions in clinical and experimental application occur principally in the lungs with grievous inflammatory and fibrotic responses (31). Although experimental pulmonary fibrosis in mice can recover in six weeks after the injury (32), intratracheal instillation of BLM causes alveolar cell destruction, inflammatory responses, EMT and subsequent ECM deposition, resembling human IPF (33). Our previous research has shown that BMP4 deficiency accelerates cellular senescence and defective mitophagy of lung fibroblasts and promotes lung fibrosis in mice (23). However, it remained uncertain whether BMP4 directly affects the degree of BLM-induced activation of NLRP3 inflammasome and EMT in AECs. We illustrated that BMP4 was markedly decreased in the lung of BLM-induced murine pulmonary fibrosis. We illustrated substantially by using histochemistry, and biochemical analysis, that genetic deletion of BMP4 accelerated BLM-induced pulmonary fibrosis, whereas AAV9-BMP4 ameliorated BLM-induced pulmonary fibrosis in mice. BMP4 could efficiently inhibit BLM-induced NLRP3 inflammasome activation and EMT process *in vitro* and *in vivo* via ERK1/2 signaling pathway, which greatly deepened our knowledge of BMP4 in pulmonary fibrosis.

IPF is characterized by excessive accumulation of ECM-producing myofibroblasts in the lung that damages alveolar architecture and impairs the gas exchange capacity of the lung (34). Although the pathogenesis of IPF remains largely ill-defined, AECs, especially type II AECs, have been considered to function as adult stem cells in the lungs (11). Growing evidence supports the notion that reiterant damage to the AECs is usually the "prime mover" for pulmonary fibrosis (26,35). Increasing evidence has shown that NLRP3 is not only present in immune cells, fibroblasts, but also found in AECs (27,36-38). NLRP3 inflammasome activation has been shown to play an important role in many respiratory diseases including IPF and the BLM model for lung fibrosis by amplifying the pro-inflammatory response cascade (7,8,11). For instance, NLRP3 inflammasomes can activate caspase-1, leading to the maturation of IL-18

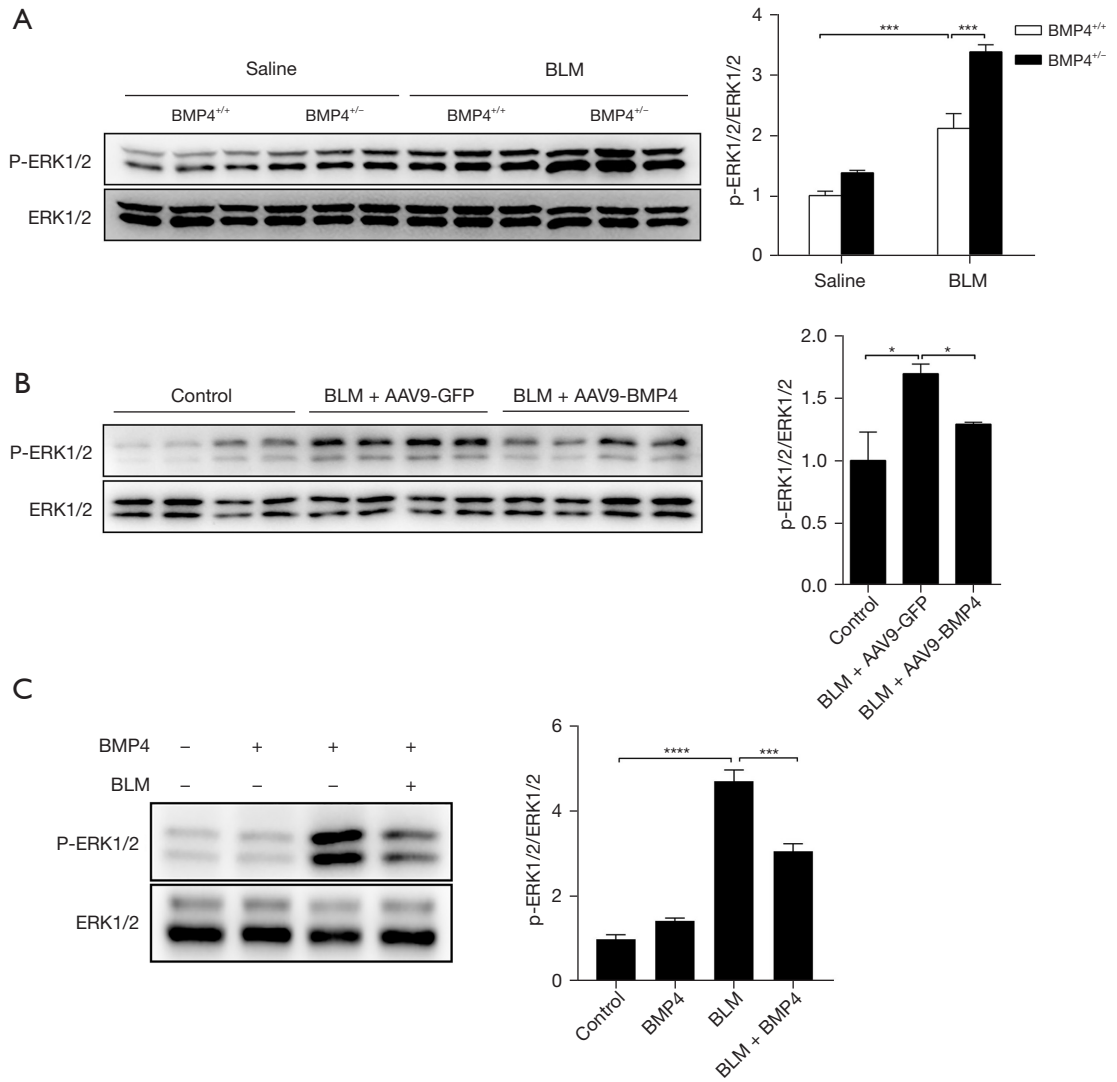

Figure 7 Effects of BMP4 on BLM-induced ERK1/2 signaling activation *in vivo* and *in vitro*. (A) *BMP4*$^{+/+}$ and *BMP4*$^{+/-}$ mice were challenged with intratracheal BLM and analyzed after 21 days. Western blot of phosphorylated and total ERK1/2 in the lung homogenates of BLM-challenged *BMP4*$^{+/+}$ and *BMP4*$^{+/-}$ mice. β-actin was used as a loading control. Data are presented as the mean ± SEM, n=6. (B) Mice were intratracheally injected with BLM, and were subsequently intratracheally injected with AAV9-BMP4 or AAV9-GFP on day 10. Western blot of phosphorylated and total ERK1/2 in the lung homogenates of AAV9-BMP4- or AAV9-GFP-treated mice. β-actin was used as a loading control. Data are presented as the mean ± SEM, n=4. (C) Western blot analysis of phosphorylated and total ERK1/2 in total cell lysates of A549 cells treated with BLM (50 μg/mL, 48 h) in the presence of BMP4 or vehicle. Data are presented as the mean ± SEM, n=3. *, P<0.05; ***, P<0.001; ****, P<0.0001. BLM, bleomycin; SEM, standard error of mean.

and IL-1β and the subsequent induction of pyroptosis (8). NLRP3 inflammasome activation has also been reported to be involved in the regulation of EMT in BLM-induced lung fibrosis, and neutralization of IL-18 could attenuate the BLM-induced lung fibrosis by inhibiting EMT (14,39). Therefore, the inhibition of NLRP3 inflammasome activation can attenuate pulmonary fibrosis. Here, we for the first time reported that BMP4 reduced BLM-induced pulmonary fibrosis via suppressing NLRP3 inflammasome activation *in vivo* and *in vitro*. Our results are in accordance with previous studies showing that BMP4 was negatively correlated with NLRP3 in white adipose tissue (40), and

that BMP4 governs an anti-inflammatory program in atherosclerosis and acute lung injury (19,22). Our results support a role for NLRP3 inflammasome activation in pulmonary fibrosis and show that BMP4 can inhibit BLM-induced NLRP3 inflammasome activation, thereby preventing the development of pulmonary fibrosis. Up till now, we first report that BMP4 suppresses the activation of NLRP3 inflammasome during pulmonary fibrosis.

After lung injury, the surviving AECs in the IPF lungs show a alterations of cell phenotype via EMT (41,42). Accumulating evidence suggests that EMT, a phenotypic plasticity process which confers migratory and invasive properties to epithelial cells, is not only a critical driving factor for the fibrotic diseases, but also a primary source of fibroblasts/myofibroblast in the development of pulmonary fibrosis (28,43). Previous research has shown that approximately 33% of myofibroblasts in an experimental mouse model of lung fibrosis can be traced to cells undergoing EMT. For instance, immunohistochemistry staining of IPF lung tissues showed an extended E-cadherin expression into the basal cells, where N-cadherin and vimentin protein expression levels were enhanced, implying that AECs were in the process of cell phenotype transdifferentiation into mesenchymal cells (42). Hence, EMT is identified as a fundamental pathogenesis in fibrotic lungs. In the present study, we found that the mouse lungs underwent EMT after BLM, as demonstrated by phenotypic and biomarker changes, which is in accordance with previous observations (7,8). Whereas BMP4 significantly inhibited BLM-induced EMT in the lungs, further indicating the anti-fibrotic role of BMP4 in pulmonary fibrogenesis. This is in line with previous findings that BMP4 represses EMT in proliferative vitreoretinopathy, peritoneal fibrosis and kidney fibrosis (21,44,45). Additionally, in recent years, more and more studies have reported that, over and above the TGF-β1, BLM can directly trigger EMT in both primary AECs and alveolar epithelial A549 cell line (11). Consistently, our data certified that BLM successfully induced EMT in alveolar A549 cells, and BMP4 treatment significantly inhibited BLM-induced EMT as demonstrated by the alteration of EMT-related biomarkers. These results suggest that BMP4 ameliorates pulmonary fibrosis by inhibiting EMT.

As an important member of the TGF-β superfamily, BMP4 can bind to its receptor to activate downstream signaling pathways, for example, ERK1/2 signaling pathway, which has been demonstrated to be able to induce NLRP3 inflammasome activation and EMT in cells in response to stress stimuli (46-48). Evidence implicates that ERK1/2 signaling pathway is involved in NLRP3 inflammasome activation and EMT in pulmonary fibrosis (34,49). In this study, we demonstrated that the protective effect of BMP4 in AECs is related to the inactivation of ERK1/2 signaling, which is in line with a previous finding (21). These above observations confirm that BMP4 overexpression can restrain the development of pulmonary fibrosis.

Conclusions

In conclusion, our study demonstrated that BMP4 reduces BLM-induced NLRP3 inflammasome activation and EMT process in AECs and eventually attenuates lung fibrosis by suppressing ERK1/2 signaling pathway. Therefore, the findings give evidence of the therapeutic potential of BMP4 gene therapy to effectively improve lung fibrosis in human.

Acknowledgments

Funding: This work was supported by grants from the Guangzhou Municipal Science and Technology Project (Nos. 202102010286, 2024B03J1383, 201804010052 and 202102020130), the National Natural Science Foundation of China (Nos. 82330002, 82241026, 81770043, 81703792, 81800072, 81900755 and 81520108001), the Local Innovative and Research Teams Project of Guangdong Pearl River Talents Program (No. 2017BT01S155), the Natural Science Foundation of Guangdong Province (Nos. 2018A030310291 and 2016A030311020), the Changjiang Scholars and Innovative Research Team in University Grant (No. IRT0961), the Health Commission of Shanghai Municipality (No. 20194Y0384), and Guangzhou national Lab Project (No. GZNL2023A02006).

Footnote

Reporting Checklist: The authors have completed the ARRIVE reporting checklist. Available at https://jtd.amegroups.com/article/view/10.21037/jtd-23-1947/rc

Data Sharing Statement: Available at https://jtd.amegroups.com/article/view/10.21037/jtd-23-1947/dss

Peer Review File: Available at https://jtd.amegroups.com/

article/view/10.21037/jtd-23-1947/prf

Conflicts of Interest: All authors have completed the ICMJE uniform disclosure form (available at https://jtd.amegroups.com/article/view/10.21037/jtd-23-1947/coif). J.H. serves as Executive Editor-in-Chief of *Journal of Thoracic Disease*. The other authors have no conflicts of interest to declare.

Ethical Statement: The authors are accountable for all aspects of the work in ensuring that questions related to the accuracy or integrity of any part of the work are appropriately investigated and resolved. A protocol for animal experiments was prepared before the study with registration in the Animal Care and Use Committee of Guangzhou Medical University. Animal experiments were performed under a project license (No. 2021433) granted by the Animal Care and Use Committee of Guangzhou Medical University, in compliance with institutional guidelines for the care and use of animals.

References

1. Raghu G, Collard HR, Egan JJ, et al. An official ATS/ERS/JRS/ALAT statement: idiopathic pulmonary fibrosis: evidence-based guidelines for diagnosis and management. Am J Respir Crit Care Med 2011;183:788-824.
2. Muthuramalingam K, Cho M, Kim Y. Cellular senescence and EMT crosstalk in bleomycin-induced pathogenesis of pulmonary fibrosis-an in vitro analysis. Cell Biol Int 2020;44:477-87.
3. Andugulapati SB, Gourishetti K, Tirunavalli SK, et al. Biochanin-A ameliorates pulmonary fibrosis by suppressing the TGF-β mediated EMT, myofibroblasts differentiation and collagen deposition in in vitro and in vivo systems. Phytomedicine 2020;78:153298.
4. Chen YL, Zhang X, Bai J, et al. Sorafenib ameliorates bleomycin-induced pulmonary fibrosis: potential roles in the inhibition of epithelial-mesenchymal transition and fibroblast activation. Cell Death Dis 2013;4:e665.
5. Li J, Liu J, Yue W, et al. Andrographolide attenuates epithelial-mesenchymal transition induced by TGF-β1 in alveolar epithelial cells. J Cell Mol Med 2020;24:10501-11.
6. Gao F, Zhang Y, Yang Z, et al. Arctigenin Suppressed Epithelial-Mesenchymal Transition Through Wnt3a/β-Catenin Pathway in PQ-Induced Pulmonary Fibrosis. Front Pharmacol 2020;11:584098.
7. Li J, Yang X, Yang P, et al. Andrographolide alleviates bleomycin-induced NLRP3 inflammasome activation and epithelial-mesenchymal transition in lung epithelial cells by suppressing AKT/mTOR signaling pathway. Ann Transl Med 2021;9:764.
8. Peng L, Wen L, Shi QF, et al. Scutellarin ameliorates pulmonary fibrosis through inhibiting NF-κB/NLRP3-mediated epithelial-mesenchymal transition and inflammation. Cell Death Dis 2020;11:978.
9. Strieter RM. What differentiates normal lung repair and fibrosis? Inflammation, resolution of repair, and fibrosis. Proc Am Thorac Soc 2008;5:305-10.
10. Moossavi M, Parsamanesh N, Bahrami A, et al. Role of the NLRP3 inflammasome in cancer. Mol Cancer 2018;17:158.
11. Tian R, Zhu Y, Yao J, et al. NLRP3 participates in the regulation of EMT in bleomycin-induced pulmonary fibrosis. Exp Cell Res 2017;357:328-34.
12. Lasithiotaki I, Giannarakis I, Tsitoura E, et al. NLRP3 inflammasome expression in idiopathic pulmonary fibrosis and rheumatoid lung. Eur Respir J 2016;47:910-8.
13. Zheng R, Tao L, Jian H, et al. NLRP3 inflammasome activation and lung fibrosis caused by airborne fine particulate matter. Ecotoxicol Environ Saf 2018;163:612-9.
14. Song C, He L, Zhang J, et al. Fluorofenidone attenuates pulmonary inflammation and fibrosis via inhibiting the activation of NALP3 inflammasome and IL-1β/IL-1R1/MyD88/NF-κB pathway. J Cell Mol Med 2016;20:2064-77.
15. Abd Elrazik NA, Helmy SA. Betanin protects against bleomycin-induced pulmonary fibrosis by regulating the NLRP3/IL-1β/TGF-β1 pathway-mediated epithelial-to-mesenchymal transition. Food Funct 2024;15:284-94.
16. Davis H, Raja E, Miyazono K, et al. Mechanisms of action of bone morphogenetic proteins in cancer. Cytokine Growth Factor Rev 2016;27:81-92.
17. Shu DY, Ng K, Wishart TFL, et al. Contrasting roles for BMP-4 and ventromorphins (BMP agonists) in TGFβ-induced lens EMT. Exp Eye Res 2021;206:108546.
18. Zhu D, Wu J, Spee C, et al. BMP4 mediates oxidative stress-induced retinal pigment epithelial cell senescence

and is overexpressed in age-related macular degeneration. J Biol Chem 2009;284:9529-39.
19. Zuo WL, Yang J, Strulovici-Barel Y, et al. Exaggerated BMP4 signalling alters human airway basal progenitor cell differentiation to cigarette smoking-related phenotypes. Eur Respir J 2019;53:1702553.
20. Li Z, Wang J, Wang Y, et al. Bone morphogenetic protein 4 inhibits liposaccharide-induced inflammation in the airway. Eur J Immunol 2014;44:3283-94.
21. Yao H, Li H, Yang S, et al. Inhibitory Effect of Bone Morphogenetic Protein 4 in Retinal Pigment Epithelial-Mesenchymal Transition. Sci Rep 2016;6:32182.
22. Mu W, Qian S, Song Y, et al. BMP4-mediated browning of perivascular adipose tissue governs an anti-inflammatory program and prevents atherosclerosis. Redox Biol 2021;43:101979.
23. Guan R, Yuan L, Li J, et al. Bone morphogenetic protein 4 inhibits pulmonary fibrosis by modulating cellular senescence and mitophagy in lung fibroblasts. Eur Respir J 2022;60:2102307.
24. Ashcroft T, Simpson JM, Timbrell V. Simple method of estimating severity of pulmonary fibrosis on a numerical scale. J Clin Pathol 1988;41:467-70.
25. Guan R, Cai Z, Wang J, et al. Hydrogen sulfide attenuates mitochondrial dysfunction-induced cellular senescence and apoptosis in alveolar epithelial cells by upregulating sirtuin 1. Aging (Albany NY) 2019;11:11844-64.
26. Sakai N, Tager AM. Fibrosis of two: Epithelial cell-fibroblast interactions in pulmonary fibrosis. Biochim Biophys Acta 2013;1832:911-21.
27. Liu W, Han X, Li Q, et al. Iguratimod ameliorates bleomycin-induced pulmonary fibrosis by inhibiting the EMT process and NLRP3 inflammasome activation. Biomed Pharmacother 2022;153:113460.
28. King TE Jr, Pardo A, Selman M. Idiopathic pulmonary fibrosis. Lancet 2011;378:1949-61.
29. Raghu G. Epidemiology, survival, incidence and prevalence of idiopathic pulmonary fibrosis in the USA and Canada. Eur Respir J 2017;49:1602384.
30. Phan THG, Paliogiannis P, Nasrallah GK, et al. Emerging cellular and molecular determinants of idiopathic pulmonary fibrosis. Cell Mol Life Sci 2021;78:2031-57.
31. Song N, Liu J, Shaheen S, et al. Vagotomy attenuates bleomycin-induced pulmonary fibrosis in mice. Sci Rep 2015;5:13419.
32. Degryse AL, Lawson WE. Progress toward improving animal models for idiopathic pulmonary fibrosis. Am J Med Sci 2011;341:444-9.
33. Moore BB, Hogaboam CM. Murine models of pulmonary fibrosis. Am J Physiol Lung Cell Mol Physiol 2008;294:L152-60.
34. Guan R, Wang X, Zhao X, et al. Emodin ameliorates bleomycin-induced pulmonary fibrosis in rats by suppressing epithelial-mesenchymal transition and fibroblast activation. Sci Rep 2016;6:35696.
35. Min L, Shu-Li Z, Feng Y, et al. NecroX-5 ameliorates bleomycin-induced pulmonary fibrosis via inhibiting NLRP3-mediated epithelial-mesenchymal transition. Respir Res 2022;23:128.
36. Liang Q, Cai W, Zhao Y, et al. Lycorine ameliorates bleomycin-induced pulmonary fibrosis via inhibiting NLRP3 inflammasome activation and pyroptosis. Pharmacol Res 2020;158:104884.
37. Liu Y, Chen S, Yu L, et al. Pemafibrate attenuates pulmonary fibrosis by inhibiting myofibroblast differentiation. Int Immunopharmacol 2022;108:108728.
38. Ji J, Hou J, Xia Y, et al. NLRP3 inflammasome activation in alveolar epithelial cells promotes myofibroblast differentiation of lung-resident mesenchymal stem cells during pulmonary fibrogenesis. Biochim Biophys Acta Mol Basis Dis 2021;1867:166077.
39. Zhang LM, Zhang Y, Fei C, et al. Neutralization of IL-18 by IL-18 binding protein ameliorates bleomycin-induced pulmonary fibrosis via inhibition of epithelial-mesenchymal transition. Biochem Biophys Res Commun 2019;508:660-6.
40. Cao W, Huang H, Xia T, et al. Homeobox a5 Promotes White Adipose Tissue Browning Through Inhibition of the Tenascin C/Toll-Like Receptor 4/Nuclear Factor Kappa B Inflammatory Signaling in Mice. Front Immunol 2018;9:647.
41. Li Q, Deng MS, Wang RT, et al. PD-L1 upregulation promotes drug-induced pulmonary fibrosis by inhibiting vimentin degradation. Pharmacol Res 2023;187:106636.
42. Hill C, Jones MG, Davies DE, et al. Epithelial-mesenchymal transition contributes to pulmonary fibrosis via aberrant epithelial/fibroblastic cross-talk. J Lung Health Dis 2019;3:31-5.
43. Su J, Morgani SM, David CJ, et al. TGF-β orchestrates fibrogenic and developmental EMTs via the RAS effector RREB1. Nature 2020;577:566-71. Erratum in: Nature 2020;578:E11.
44. Leung JC, Chan LY, Tam KY, et al. Regulation of CCN2/CTGF and related cytokines in cultured peritoneal cells under conditions simulating peritoneal dialysis. Nephrol Dial Transplant 2009;24:458-69.

45. Mason RM. Fell-Muir lecture: Connective tissue growth factor (CCN2) -- a pernicious and pleiotropic player in the development of kidney fibrosis. Int J Exp Pathol 2013;94:1-16.
46. Yuan L, Zhu Y, Huang S, et al. NF-κB/ROS and ERK pathways regulate NLRP3 inflammasome activation in Listeria monocytogenes infected BV2 microglia cells. J Microbiol 2021;59:771-81.
47. Zhang X, Huang S, Zhuang Z, et al. Lipin2 ameliorates diabetic encephalopathy via suppressing JNK/ERK-mediated NLRP3 inflammasome overactivation. Int Immunopharmacol 2023;118:109930.
48. Yang YC, Chien Y, Yarmishyn AA, et al. Inhibition of oxidative stress-induced epithelial-mesenchymal transition in retinal pigment epithelial cells of age-related macular degeneration model by suppressing ERK activation. J Adv Res 2024;60:141-57.
49. Colunga Biancatelli RML, Solopov P, Dimitropoulou C, et al. Age-Dependent Chronic Lung Injury and Pulmonary Fibrosis following Single Exposure to Hydrochloric Acid. Int J Mol Sci 2021;22:8833.

Cite this article as: Xu X, Yuan L, Hu X, Li J, Wu H, Chen F, Huang F, Kong W, Liu W, Xu J, Zhou Y, Zou Y, Shen Y, Guan R, He J, Lu W. Bone morphogenetic protein 4 ameliorates bleomycin-induced pulmonary fibrosis in mice by repressing NLRP3 inflammasome activation and epithelial-mesenchymal transition. J Thorac Dis 2024;16(8):4875-4891. doi: 10.21037/jtd-23-1947